Erklärung zur Abschlussarbeit gemäß § 22 Abs. 7 APB TU Darmstadt

Hiermit erkläre ich, Jan Kröger, dass ich die vorliegende Arbeit gemäß § 22 Abs. 7 APB der TU Darmstadt selbstständig, ohne Hilfe Dritter und nur mit den angegebenen Quellen und Hilfsmitteln angefertigt habe. Ich habe mit Ausnahme der zitierten Literatur und anderer in der Arbeit genannter Quellen keine fremden Hilfsmittel benutzt. Die von mir bei der Anfertigung dieser wissenschaftlichen Arbeit wörtlich oder inhaltlich benutzte Literatur und alle anderen Quellen habe ich im Text deutlich gekennzeichnet und gesondert aufgeführt. Dies gilt auch für Quellen oder Hilfsmittel aus dem Internet.

Diese Arbeit hat in gleicher oder ähnlicher Form noch keiner Prüfungsbehörde vorgelegen.

Mir ist bekannt, dass im Falle eines Plagiats (§ 38 Abs. 2 APB) ein Täuschungsversuch vorliegt, der dazu führt, dass die Arbeit mit 5,0 bewertet und damit ein Prüfungsversuch verbraucht wird. Abschlussarbeiten dürfen nur einmal wiederholt werden.

Bei einer Thesis des Fachbereichs Architektur entspricht die eingereichte elektronische Fassung dem vorgestellten Modell und den vorgelegten Plänen.

Darmstadt, 10. Oktober 2023

J. Kröger

Contents

1 Introduction **5**

2 Wetting Theory **8**
2.1 Surface Tension 8
2.2 Wetting Phenomenon 9
2.2.1 Dynamic Weting 10
2.2.2 Capillary Rise 12
2.3 Simulating the Wetting Processes 15

3 Phase Field Method **17**
3.1 Phase Field Method in the Spirit of Cahn and Hillard 18
3.1.1 Mixing Energy 18
3.1.2 Diffusive Interaface 19
3.1.3 Wall Energy 19
3.2 Cahn-Hillard Navier Stokes Equations 20

4 Case Setup **21**
4.1 Discretization 22

5 Validation **23**

6 Results **24**

7 Outlook **25**

Todo list

ADD CHAPTER 6

ADD CHAPTER 6

Here a introduction, but probably only after the most is done and the layout of the thesis is set. 6

check if quere1997 is also a source. Probably talked about that. Maybe even Washburn talked about that? 6

rework this regment. 6

ref chapter 7

ref chapter 7

ref to both chapters 7

chapter 7

chapter 7

mention that we are considering spontaneous cap rise (no pressure or something like that) 8

ref 8

ref 8

ref chapter 8

ref 8

rework 8

possibly ref to corresponding chapters here. 8

ref 9

ref; i think it was butt 9

cite lacis 11

cite papers. look it up you had some. 14

maybe use this eq instead of shorted one? 15

Elaborate or maybe move the entire section to phase field? Or perhaps case setup with a reasoning why phase field? 16

ref chapter PhaseField 17

einleitende Worte 17

picture of interfaces 17

check!!! 18

check if right function 18

check if already mentioned 18

cite 18

cite 20

insert table 21

add checcks which were made; Viscosity scheme, probes, funkysetfields, preconditioner, boundary conditions, n cores decomposition 21

elaborate 21

ref to chapter ooEBC 22

we used an other geometry. How do i write it then?new image with new text? . . . 22

bodziony2023, Cai2015, woerner2021, Samkhaniani2021, holtzinger, marianna?, hagg?(sogar mit wedge und amr) 23

The Position of the meniskus was exported with paraview in the decomposed state. The position was then extracted with a python script.Probe data was preprocessed as well and several computations for eval of simulations. Plots were generated with matplotlib?; Start of real results with an overview when what where. Maybe work with normalized data? 24

1 Introduction

Many everyday phenomena that we observe are, contrary to expectations, not yet fully understood. This does not mean that they are not utilized in a variety of technical devices. In the case of wetting, we encounter many different things in everyday life, such as a drop on a window pane that seems to slide down randomly, or the sleeve of a sweater that seems to soak up water when washing hands.

Nature has a head start in this effect and has produced creatures that can walk on water because they take advantage of the water's surface tension. The flora also uses surface tension, whether it's trees that wouldn't reach the size we know without the capillary effect, or the lotus flower, which, with its water-repellent (hydrophobic) surface, ensures that water rolls off and takes dirt with it in the process.

Porous media, through their use in oxygenators, became lifesavers during the Corona pandemic by reoxygenating blood. The potential applications and necessities of this phenomenon could be demonstrated with many more examples. This work aims to describe the dynamics of capillary rise through simulations. A porous medium can be simplified as a collection of many small tubes. Insights from these small tubes can then be extrapolated to determine the behavior of the porous medium. Therefore, experiments with both porous media and individual capillaries are of great interest to understand how the rise in the capillary is designed. Simulations of these processes are also increasingly being carried out, as they have the advantage of fixing certain relevant material properties to examine their influence, or to look into areas that would not be possible with a conventional experimental setup.

In this work, the rise of a liquid column (water) in a capillary is investigated. Specifically, for a two-phase system, the area around the interface in the water phase is examined, and how dissipative processes in this region influence the rise of the water column. Possible phase changes (evaporation, boiling, condensation, etc.) are not taken into account. An isothermal and isobaric system is also assumed. All fluids treated are Newtonian, and the flow can be assumed to be Poiseuille flow. Furthermore, newly implemented boundary conditions of the used solver, which are supposed to better represent the behavior of the contact line and contact angle, will also be checked.

This work will first discuss important findings in the description of capillary rise, the contact line, and the simulation of such problems with phase field methods in Chapter **??**. This is followed by an overview of the important influencing factors of wetting and

their influence on the topics discussed in Chapter 2. Chapter 3 provides an introduction to the phase field method and how it is implemented to simulate such problems. Chapter 5 shows that the solver used has already shown in many other simulations that it produces correct results and is applicable to these problems. Validation of the geometries used here is not possible due to their size, as they have a radius of 3 nm. It is not currently known that there are experiments that provide reliable results with a constant cross-section and such small radii. Subsequently, Chapter 4 describes the setup of the simulations with descriptions of the geometry, material properties used, and solver settings. Finally, the results are discussed in Chapter , and an outlook for upcoming investigations is given in Chapter .

ADD CHAPTER

ADD CHAPTER

The solver used here is `phaseFieldFoam`, which is an extension of the open-source environment `OpenFOAM-extend`. The version used of `OpenFOAM-extend` is 5.0, and the version of the solver is still in development. The further development and maintenance of the solver are carried out through a cooperation between KIT (Karlsruhe Institute of Technology) and TU Darmstadt, especially by Dr.-Ing. Xuan Cai and Dr.-Ing. Holger Marschall. The simulations for this research were conducted on the Lichtenberg high-performance computer of the TU Darmstadt.

Here a introduction, but probably only after the most is done and the layout of the thesis is set.

The dynamics of a rising fluid in the capillary is the subject of many processes. In nature, for example, trees would not be able to grow as high as they do without the capillary effect, and in technology many processes with a porous medium exist. Porous media can be simplified as many small tubes through which a fluid travels. Therefore, this process has long been of great interest in science and yet there are many uncertainties in the description of the dynamics.

The Lucas Washburn equation, introduced in 1921 [**lucas_ueber_1918**, **washburn_dynamics_1921**], attempts to describe the height of the propagating fluid column as a function of time. This equation is sufficiently accurate for many applications.

However, due to the assumptions made in the derivation of the equation, it is clear that it cannot be applied to every problem. Therefore, there are many approaches to adapt this equation to problems and simply maintain the behaviour of the equation.

It is shown, that the Lucas Washburn equation has its problems in early stages of the imbibition[**bosanquet_lv_1923**, **quere_inertial_1997**], due to the undefined behaviour for $t = 0$ and neglecting the inertia of the fluid.

check if quere1997 is also a source. Probably talked about that. Maybe even Washburn talked about that?

The early stages of the imbibition process is yet to be understood and in this work we show how the different forces are acting on the meniscus for small time steps with a simulation of the such a problem. This simulations are done with the open source framework of foam extend, which is a fork of open foam. Here the department of mathmatics of the TU Darmstadt and the KIT developed a solver for a phase field approach.

rework this regment.

The developed solver phaseFieldFoam is maintained and developed by the department of MMA at the Tu darmstadt and ... KIT. It is using the Phase field approach to solve the Navier Stokes Equations (NSE).

In this work, first the attempts to describe the imbibition of a fluid in a capillay, especially for the early stages and small capillaies are discussed. Followed by the work, which has been done to simulate such problems with the phase field approach. Important interrelationships and derivations of the process of wetting is discussed, again followed by the equivalent numerical relations. How the simulations are setup and the results are in the chapers and .

ref chapter

ref chapter

ref to both chapters

chapter

chapter

Lucas needed to prewet the tube to get the results he predicted

In this work

2 Wetting Theory

The wetting theory describes the interaction of fluids with solid surfaces. Many processes in nature, as well as in technology, are affected by this phenomenon. In this work, the focus is on the wetting properties in capillaries, which are often used as a simplification for understanding porous media or in other processes, such as the fact that trees would not be as tall as they are today without this effect.

First, an overview of some types of wetting is presented , and the concepts of contact angle and contact line are introduced. Subsequently, the surface tension and its role in wetting are discussed. Since this work considers the dynamic rise of a water column in a capillary, the dynamic contact angle is also examined in Chapter , followed by a description of the capillary effect and its significance for the rise of a fluid in a capillary.

mention that we are considering spontaneous cap rise (no pressure or something like that)

2.1 Surface Tension

Surface tension plays a significant role in the wetting of surfaces or in capillary rise. Therefore, it is essential to first clarify what surface tension is. In general, surface tension is a proportionality constant that depends on temperature, pressure, and the phases involved but is independent of the surface [5]. The interface separates the phases and can be interpreted differently. On a molecular level, molecules attract each other (cohesion). The interaction between two phases is called adhesion. In the case of the interaction between a liquid and a solid, adhesion can usually be neglected. In Figure 2.1, a water droplet surrounded by air is illustrated on the left. The black outer line thus represents the interface between the droplet and the air. If one now magnifies the transition area down to the molecular level (red area), one obtains the schematic representation on the right side. The blue circles are simplified representations of the water molecules, and the gray ones represent the surrounding air. Here, it is evident how, at the interface, the water molecules are no longer surrounded only by other water molecules, which is energetically unfavorable. However, since the system strives to transition into an energetically favorable state, it attempts to minimize the number of molecules lying at the interface [5].

ref

ref

ref chapter

ref

rework

possibly ref to corresponding chapters here.

To increase the surface area, molecules must be transported to the surface, and energy must be supplied to the system. Therefore, surface tension is also interpreted as the

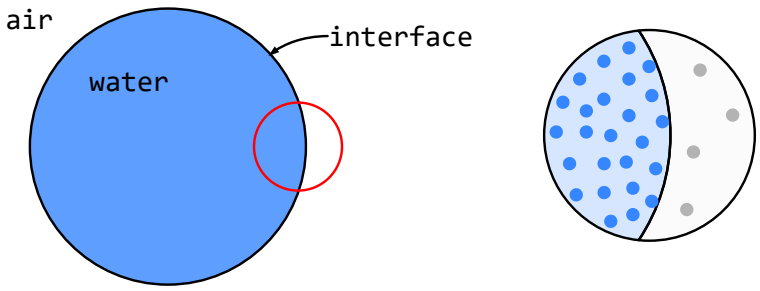

Figure 2.1: Schematic of interacting molecules in a liquid droplet and its interaction with a vapor

necessary energy required to carry a molecule to the surface.

$$dE = \sigma \cdot dA \tag{2.1}$$

with dE as the supplied energy and dA as the change in surface area.

2.2 Wetting Phenomenon

Despite the fact that the wetting of droplets is not considered in this work, it is appropriate to describe the fundamentals of wetting using this example. The concepts are the same, and many initial studies are based on this example.

In the case where the system is in equilibrium, Young derived an equation relating surface tensions to the contact angle:

ref

$$\sigma_{\mathrm{LV}} \cdot \cos\theta_{\mathrm{e}} = \sigma_{\mathrm{SV}} - \sigma_{\mathrm{SL}} \tag{2.2}$$

Where σ_{LV} is the surface tension between the liquid and the gas, σ_{SV} is from the solid to the gas, and σ_{SL} is between the solid and the liquid (see Figure 2.2). If $(\sigma_{\mathrm{SV}} > \sigma_{\mathrm{SL}})$ holds true, a contact angle less than $90°$ follows; otherwise, $90° \leq \theta_{\mathrm{e}} < 180°$. In the case where $\sigma_{\mathrm{SV}} = \sigma_{\mathrm{SL}} + \sigma_{\mathrm{LV}}$, complete wetting of the surface occurs [5].

When a droplet impacts a solid surface, different states can arise depending on the fluid-solid combination. At the point where the interface of the two fluids (droplet and surrounding fluid) meets the solid surface, the contact line is formed (see 2.2; red line). Depending on the fluid-fluid-solid combination, a contact angle θ_{e} is established, where the suffix e stands for equilibrium. In the case of complete wetting, the fluid spreads over the entire surface (see Figure 2.3 a)). This effect, however, is challenging to reproduce as it can be hindered by surface irregularities . As seen in Figure 2.3(b-d)), states where a droplet forms on the surface are further subdivided. For a contact angle $\theta_{\mathrm{e}} < 90°$, it is

ref; i think it was butt

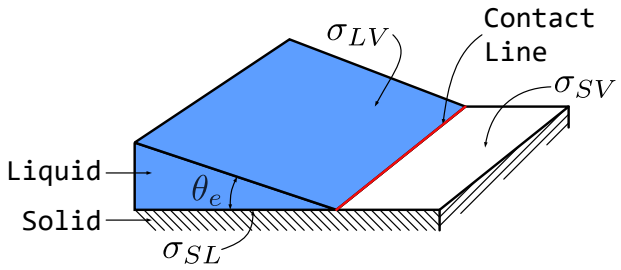

Figure 2.2: Three Phase Contact Line

termed hydrophilic (see 2.3b)), for $\theta_e > 90°$ it's hydrophobic (see 2.3c)), and for a contact angle $\theta_e > 120°$, it's superhydrophobic surfaces (see 2.3d)). Developing superhydrophobic surfaces is also challenging. To curve the surface of the liquid, a pressure difference must

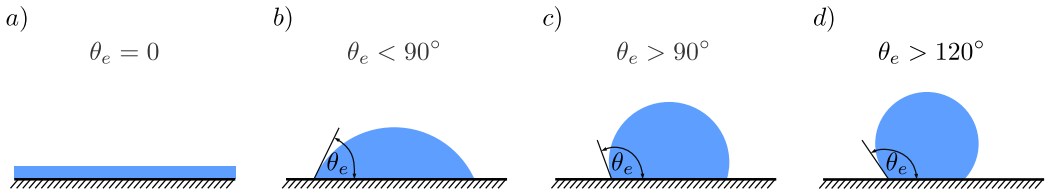

Figure 2.3: Wetting of a surface

exist. In the case of a sphere, Young and Laplace developed a relationship for the pressure difference in terms of the surface tension and radius as:

$$P_\mathrm{i} - P_\mathrm{o} = \Delta P = \frac{2\sigma}{R} \tag{2.3}$$

With ΔP being the pressure difference at the interface, P_i as the pressure inside the droplet, P_o the ambient pressure, and R as the radius of the sphere. For a derivation, refer to [5].

2.2.1 Dynamic Weting

So far, only states have been considered that observe systems in equilibrium. Typically, however, the contact line is in motion. When the contact line is moving, the contact angle (dynamic contact angle θ_D) differs from that in the equilibrium state [3]. To describe the dynamics of the contact line, the dynamic contact angle, the relative speed of the contact line, and the equilibrium contact angle are required [28, 3, 10, 20, 34]. However, describing the contact line is challenging due to the fact that the microscopic level affects the macroscopic level.

In Figure 2.4, various views of the contact line are illustrated. The red circle in *a)* points to the area considered in the picture next to it and can be understood as a magnifying glass. If we enlarge the area in *a)*, we see the interpretation of the contact line from the perspective of the hydrodynamic theory, with a microscopic contact angle θ_{m} and the dynamic contact angle θ_{D} (Figure 2.4 *b)*). Focusing again on the contact line, we see the interpretation of the molecular kinetic theory (Figure 2.4 *c)*). The illustrated points are intended to represent molecules in a simplified form.

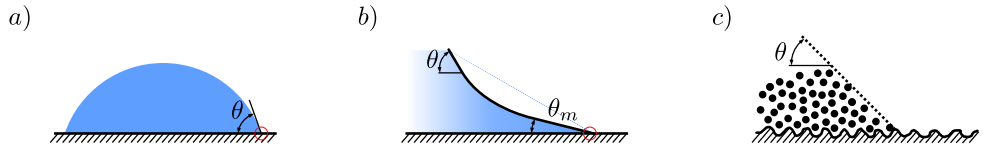

Figure 2.4: Hydrodynamic and Molecular Kinetic description of the Contact angle. Figure b) corresponds to the area circled in red in a), and c) to the area from image b).

Hydrodynamic Theory The hydrodynamic approach solves the physics of the flow using the Navier-Stokes equations but encounters a singularity at the contact line when a sticking condition is applied [20]. To address this issue, either the sticking condition near the wall was relaxed or the solution was truncated at the molecular level [3]. In both cases, a small capillary number is assumed, which means that far from the contact line, the interface assumes its equilibrium shape.

Voinov [34] derived a description of the contact line for a spreading droplet depending on the capillary number. A generalized version was developed by Cox [10] with some correction terms [8, 3]. Thus, the dynamic contact angle for $\theta_{\mathrm{D}} \leq 3/4\pi$ is given by

$$\theta_D^3 - \theta_m^3 = 9Ca \ln\left(\frac{L}{L_m}\right) = 9\frac{\mu u}{\sigma} \ln\left(\frac{L}{L_m}\right) \tag{2.4}$$

With L as the macroscopic path length and L_{m} as the microscopic path length. Assuming that the interface assumes its equilibrium shape far away, $\theta_{\mathrm{m}} = \theta_{\mathrm{e}}$. However, Voinov himself already pointed out that θ_{m} could also depend on the speed [34, 3]. cite lacis

Molecular Kinetic Theory The Molecular Kinetic Model describes the movement of the contact line with a statistical description of the molecular movement at the contact line [2]. In contrast to the hydrodynamic model, the molecular processes at the contact line influence those of the larger scales. In this view, the molecules at the contact line jump back and forth to adsorption sites on the solid substrate. The speed of the contact line is determined by multiplying the difference between the forward and backward jumps by a

jump distance λ. This results in the description

$$u = 2\lambda\kappa_0 \sinh\left(\frac{\sigma\left(\cos\theta_\mathrm{e} - \cos\theta_\mathrm{D}\right)}{2nk_\mathrm{B}T}\right). \tag{2.5}$$

Where n is the number of adsorption sites per unit area, k_0 is a characteristic frequency, k_B is the Boltzmann constant, and T is the temperature. If the system is in equilibrium, the forward and backward jumping is balanced, and the contact line comes to a standstill [7, 3]. However, a problem with this view is that this model is more qualitative and computationally intensive [28].

2.2.2 Capillary Rise

A capillary is a very thin tube in which, due to surface effects, a liquid rises or falls without external force. In 2.5, a capillary with an already risen liquid column is shown. The well-known surface tensions are also marked at their respective locations, as well as the essential geometric parameters, such as diameter ($2R$) or height of the resulting meniscus z. The resulting contact angle after reaching equilibrium, θ_e, is also shown. The system in this representation is also subject to gravitational forces.

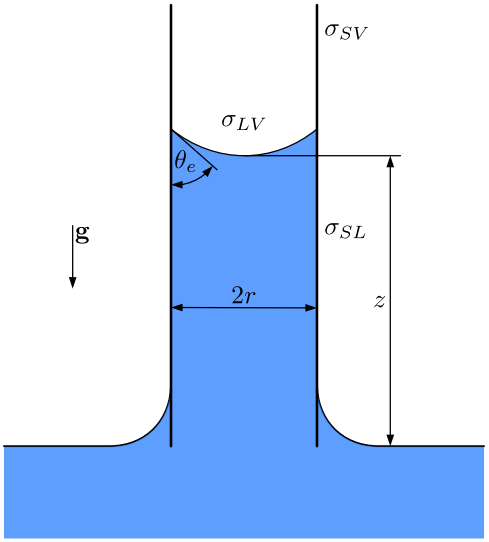

Figure 2.5: Schematic representation of a capillary in a liquid after it has penetrated the capillary.

In this work, such a system is used. However, further conditions apply. It is assumed that the system is isobaric, isothermal, and the liquid is Newtonian. Furthermore, it is assumed that while the water column rises in the capillary, a Poiseuille flow is present and no phase

change occurs. It is also assumed that the viscosity of the gas phase is negligible. With these assumptions and boundary conditions, the Newtonian dynamics in a capillary can be described as a balance between the inertial forces and the sum of the capillary forces, viscous forces, and hydrostatic forces [16]:

$$\frac{d}{dt}M(z,\dot{z}) = F_{\mathrm{w}} - F_{\eta} - F_{\mathrm{g}} \tag{2.6}$$

With $M(z,\dot{z}) = \pi r^2 \rho z \dot{z}$ as the moment, $F_{\mathrm{g}} = \pi r^2 \rho g z$ as the gravitational force, and F_{η} as the viscous resistance, which results from the assumption of the average velocity and the existing Poiseuille flow to $F_{\eta} = 8\pi\eta z\dot{z}$. With $\dot{z}$ as the average velocity. The capillary forces result from the previous description of the surface tension and the change in the surface of the meniscus with a change in the current height:

$$F_{\mathrm{w}} = \sigma\frac{dA}{dz} = \sigma 2\pi r \tag{2.7}$$

The surface tension σ here is the increase in surface energy due to the wetting of the solid wall of the capillary. Thus, $\sigma = \sigma_{\mathrm{SV}} - \sigma_{\mathrm{SL}}$. This description is already known from the Young equation (2.2). Thus, after inserting for the capillary forces:

$$F_W = \sigma_{\mathrm{LV}} \cdot \cos\theta_{\mathrm{e}} 2\pi r. \tag{2.8}$$

Thus, for equation 2.6 after insertion [16]:

$$\pi r^2 \rho \frac{d}{dt}(z\dot{z}) = \sigma_{\mathrm{LV}} \cdot \cos\theta_{\mathrm{e}} 2\pi r - 8\pi\eta z\dot{z} - \pi r^2 \rho g z. \tag{2.9}$$

Early descriptions by Bell and Cameron [1] did not describe the rise dynamics based on equation 2.9. They developed the rise dynamics from experiments according to:

$$z(t)^n = K \cdot t. \tag{2.10}$$

Both n and K are temperature-dependent constants. In 1918, Lucas [26] and in 1921, Washburn [35] derived the Lucas Washburn equation by neglecting the inertial and gravitational terms:

$$z(t) = \sqrt{\frac{r\sigma\cos\theta_{\mathrm{e}}}{2\eta}t} \tag{2.11}$$

With this, they independently developed an equation with which the capillary rise can be described based on material values and measurements. Therefore, it gained popularity

over the years. Due to the neglect of individual terms and simplifications in the system, however, this equation is not always precise. Washburn himself pointed out that to meet the prediction of the equation, he had to set up the experiments in such a way that the capillary was prewetted. Therefore, adjustments to this equation were made for various problems [13]. Wu et al. [36] examined several models and compared them with experiments. In these, however, it is always assumed that the height of the meniscus increases according to $z(t) \sim \sqrt{t}$ as well.

Bosanquet [4] hinted in his 1923 paper that equation 2.11 would lead to unphysical behavior for $t \to 0$ and also developed an equation that retained this problem but now also included inertia and can give a better prediction of the rise for early times of imbibition.

cite papers. look it up you had some.

Siegel [31] studied the rise behavior under microgravity and found a linear growth. However, he did not reach the Lucas-Washburn regime. Zhmud et al. [40] also pointed out the problems for times near 0 from equation 2.11 and described a quadratic relationship for the times when the fluid is drawn into the capillary, followed by the known Lucas-Washburn regime.

Dreyer et al. [15] studied parallel plates under microgravity and divided the rise of the meniscus into three regions. Starting with a quadratic growth, followed by a linear region, and finally the Lucas-Washburn growth. Quéré [29] showed a linear growth at the beginning by assuming that in this case only inertia plays a role. Stange [32] confirmed the three regions of Dreyer et al. [15] and derived dimensionless equations to develop transition times.

Fries et al. [17] divided the growth area into areas where different forces act. In the beginning, inertia dominates, followed by a transition area where the viscous forces take over until they finally dominate. They also developed dimensionless times at which the transition takes place.

At the point where the viscous friction and the effects of inertia or dynamic contact angle are equal, Quéré [29] and Fries et al. [17] defined the characteristic penetration length:

$$l_\mathrm{c} \propto r\sqrt{\frac{r\rho\sigma}{\mu^2}} \tag{2.12}$$

Dellanoy et al. [12] focused on early times and studied viscous fluids, confirming the influence of pre-wetting the capillary, as already mentioned by Washburn [35]. They also showed a deviation from the Lucas-Washburn regime at early times. They attributed this deviation to local viscous dissipation in the wedge region, rather than a global dissipation as assumed by Lucas and Washburn. Regarding the dynamic contact angle, they showed that the characteristic penetration length (cf. Equation 2.12) is calculated as:

$$l_\mathrm{c} \propto r \ln\left(\frac{r}{l_\mathrm{m}}\right) \tag{2.13}$$

With l_m being the microscopic length that compensates for the singularity of the contact line [10]. They further assumed that once l_c is reached, the transition to the Lucas-Washburn regime occurs.

Ruiz-Gutiérrez et al. [30] contradicted this statement in their work, showing that this transition takes longer. They argue that the effects of inertia and dynamic contact angle do not decay exponentially.

To account for this, they expanded Equation 2.9 for problems with a moving interface by introducing:

$$f(\dot{z}) \equiv \frac{\cos\theta_{\mathrm{m}} - \cos\theta_D(\dot{z})}{\cos\theta_{\mathrm{m}}} \tag{2.14}$$

With the assumption that for $u > 0$ from Equation 2.4, $\theta_{\mathrm{D}} > \theta_{\mathrm{m}}$ holds true, this function disappears for $\theta_{\mathrm{D}} \to \theta_{\mathrm{m}}$.

Now, considering the moving system, Equation 2.9 for the case studied in this work becomes:

$$\pi r^2 \rho z \frac{du}{dt} = 2\pi r\sigma\cos\theta_{\mathrm{m}} + \pi r^2\rho g z - 8\pi\sigma z\dot{z} - 2\pi r\sigma\cos\theta_{\mathrm{m}} f \tag{2.15}$$

With the first two terms as driving forces and the last two as resistance forces. The last term has been added and acts as a correction for the fact that the dynamic contact angle does not correspond to the macroscopic contact angle.

Subsequently, dimensionless quantities were introduced, and four cases were defined. Two each with a large and small Laplace number, or a large and small ratio of length scales. With the quantities used in this work, case three from Ruiz-Gutiérrez et al. [30] should apply. They predict that the quadratic regime will not occur, and the rise will begin with a linear region, eventually transitioning to the Lucas-Washburn regime.

maybe use this eq instead of shorted one?

$$\pi r^2 \rho l \frac{\mathrm{d}u}{\mathrm{d}t} = 2\pi r\gamma\cos\theta_{\mathrm{a}} + \pi r^2\rho g h - 8\pi\mu l u - \frac{3}{2}\pi r^2\rho u^2 - 2\pi r\gamma\cos\theta_{\mathrm{a}} f \tag{2.16}$$

2.3 Simulating the Wetting Processes

Simulating a two-phase flow can be achieved through several methods. Common approaches include the `Volume-of-Fluid` and the `Level-Set` methods. Both methods use a sharp interface and are based on the Hydrodynamic Theory from Chapter 2.2.1. Moreover, they are *interface capturing* methods, so they don't require recalculating the computational grid over the simulation period. Other methods that follow the interface (*interface tracking*) are also possible. One of the major drawbacks of these methods is that the moving contact line, when using the adhesion condition, depends on models [8].

Additionally, calculating the surface tension can pose a challenge. This requires computing the curvature of the surface, which can lead to relatively high numerical errors [23, 18].

The Lattice-Boltzmann Method uses collision models to describe fluid behavior. Surface tensions can be considered through modifications. There are approaches that are promising and some are comparable to the phase-field method. However, one of the biggest challenges is the limitation of density or viscosity ratios. In this work, the fluids have significantly different densities with a ratio of 1000. According to [9], the Lattice-Boltzmann Method is limited to ratios of $\mathcal{O}(10)$ and can lead to instabilities otherwise.

Another frequently used method is `Molecular Dynamic` simulations. Since individual molecules are simulated in this case, this method is only applicable to geometrically and temporally small problems without driving computational costs too high. Therefore, `Molecular Dynamic` simulations are often used for comparison or to study only small problems ([11, 25, 27, 13]).

The method used in this work is the `phase-field` method. This method models two or even multi-phase flow through the system's free energy. A more detailed description of this method and the simulations already carried out is provided in Chapter 3.

Elaborate or maybe move the entire section to phase field? Or perhaps case setup with a reasoning why phase field?

3 Phase Field Method

The phase field method, rooted in system thermodynamics, offers a solution for an interface with a finite thickness, an idea originating from van der Waals in 1893 [33]. This method models the free energy of the system and can derive a phase field method for interfacial dynamics. It offers several advantages, such as mass conservation, contact line motion, and adherence to thermodynamic laws. In contrast to the hydrodynamic theory, the contact line moves through interfacial diffusion. However, there are concerns about its validity in modeling macroscopic contact line motion, especially regarding the sharp-interface limit. Despite these concerns, meaningful results have been predicted on the macro scale that align with hydrodynamic theory and experimental observations[39, 37, 7].

Phase field simulations for macroscopic wetting typically rely on the Cahn-Hilliard equations. For slow wetting phenomena, the phase field theory has been both analytically [22] and numerically [37, 39] proven to capture such wetting physics. However, for rapid spreading of water drops, the assumption of local equilibrium may not hold. Some studies have introduced a boundary condition for wetting far from equilibrium, introducing a parameter that controls the relaxation towards equilibrium . This parameter has been interpreted in various ways, from a local friction adjacent to the contact line to a relaxation parameter at the contact line[38][8].

Phase Field Theory Die Phasenfeld theorie verwendet Ansätze beider Modelle unter verwendung der Beschreibung der freien Energie des Systems.

ref chapter Phase-Field

Daher ist es auch notwendig für die Phasenfeldmethode sowohl hydrodynamische Ansätze als auch Ansätze der Molekular Kinetik Theorie zu verwenden [3, 8].

vof and level setzt difference interface tracking and capituring?

Free energy system

einleitende Worte

Wie bereits in Kapitel 2.1 beshcrieben, gibt es unterschiedliche Möglichkeiten das Interface zu beschreiben. Hydrodynamische Modelle beschreiben das Interface so, dass am Übergang der Phasen die Stoffwerte springen. Ein Diffuses Interface hingegen, beschreibt die größen anders.

picture of interfaces

3.1 Phase Field Method in the Spirit of Cahn and Hillard

Die Phasenfeld Methode geht zurück auf die Idee von van der Waals [33], der das Interface zwischen zwei nicht mischbaren Fluiden aus Sicht der Thermodynamik beschrieben hat. Darin gehen die Material Eigenschaften kontinuierlich innerhalb einer dünnen Schicht ineinander über. Innerhalb dieser Schicht existieren beide Phasen. Darauf aufbauend haben Cahn und Hillard [24] eine Beschreibung der freien Energie in einem Volumen mit ungleicher Zusammensetzung in Abhängigkeit eines Ordnungsparameters C für Zeitabhängige Probleme abgeleitet. In geschlossener Form lautet diese

$$\partial C + \mathbf{u} \cdot \nabla C = \nabla \cdot (\kappa \nabla \phi(C)) \,. \tag{3.1}$$

Darin ist $\mathbf{u}$ die Geschwindigkeit, κ ein Diffusionskoeffizient, meist mobility genannt, und ϕ ein chemisches Potential. Der ordnungsparameter gibt an welche phase vorliegt und liegt für ein zwei phasen system zwischen -1 und 1. Die Mobilität kann mit der Péclet Zahl in Verbindung gebracht werden, die eine Verhältnis der advektiven zu diffusiven flüssen mit einer charakteristischen Weglänge (L_{char}) und Geschwindigkeit (u_{char}), sowie einem Charakterischen chemischen Potential abbildet[6, 19]. Das chemische Potential ist als Ableitung der freien Helmholz Energie bezüglich des Ordungsparameters definiert [24]. Im behandelten System kann setzt sich die gesamte freie Energie aus der Mischungsenergie und der interfacial density energy zusammen. Nach [39] ist die freie Energie des Systems durch zwei Einflüsse gegeben; definiert über das Volumen Ω und die Oberfläche $\partial\Omega$

check!!!

$$F(C, \nabla C) = \int_\Omega f_{\text{mix}}(C, \nabla C) d\mathbf{x} + \int_{\partial\Omega} f_{\text{w}}(C) dS \tag{3.2}$$

Darin ist das erste integral das der mischungsenergiedichte f_{mix} und das zweite der Wand f_w.

3.1.1 Mixing Energy

Cahn und Hillard haben eine mischungsenergie (f_{mix}) definiert, die vom Ordnungsparameter und seinem Gradienten abhängt:

$$F(C, \nabla C) = \int_\Omega f_{\text{mix}}(C, \nabla C) d\mathbf{x} = \int_\Omega \left(\frac{\lambda}{\epsilon^2} \Psi(C) + \frac{\lambda}{2} |\nabla C|^2 \right) d\mathbf{x} \tag{3.3}$$

Die integration der Mischungsenergie über den Bereich ergibt die freie Helmholz Energie des Fluidsystems und besteht aus zwei Summanden. Der erste Term trennt die Phasen voneinander ab, während der zweite Term die Phasen mischt. λ ist ein mischungsenergie Parameter, ϵ ein maß für die Dicke des Interfaces und Ψ ein Potential. Das Potential wird nach Ginzburg und Landau so gewählt, dass es zwei Minima an den stellen -1 und 1 hat und ist gegeben mit

check if right function

check if already mentioned

cite

$$\Psi(C) = \frac{1}{4} \left(C^2 - 1 \right)^2 . \tag{3.4}$$

Daraus folgt die folgende Darstellung für das chemische Potential

$$\Phi(C) := \frac{\partial F(C)}{\partial C} = \frac{\lambda}{\epsilon^2}\Psi'(C) - \lambda\nabla^2 C. \tag{3.5}$$

3.1.2 Diffusive Interaface

Das Cahn Hillard Modell kann Systeme mit mehreren Fluiden beschreiben. In dieser Arbeit wird jedoch nur ein binäres Fluidsystem betrachtet. In Abbildung 3.1 ist die Kontakilinie

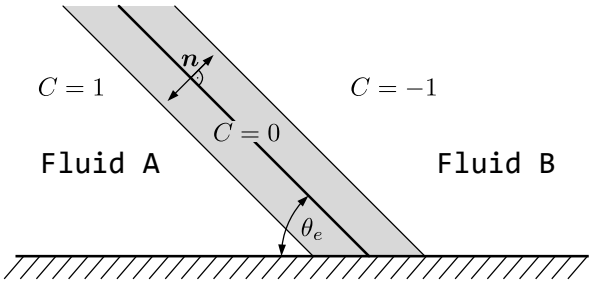

Figure 3.1: Schematische Darstellung eines Diffusiven Interfaces

eines Diffusiven interfaces dargestellt. Der Graue bereich ist der transitionsbereich des Ordnungsparameters und damit der Stoffgrößen. Innerhalb dieses Bereichs koexistieren beide Fluide mit ihren jeweiligen Dichten und viskositäten. Im Gleichgewichtszustand kann das Profil von C normal zum Interface ermittelt werden, in dem die freie Energie (Gleichung 3.5)minimiert wird [6]. Dies führt dann zu einer Beschreibung des Ordnungsparameters normal zum Interface mit

$$C(n) = \tanh\left(\frac{n}{\sqrt{2}\epsilon}\right). \tag{3.6}$$

Darin ist n die normale auf dem Interface. Im gleichgewicht bleibt die Dicke des diffusen Interfaces gleich in einem Bereich von $3/\sqrt{2}\epsilon$ gilt für den Ordnungsparameter $-0.9 \leq C \leq 0.9$. Ebenfalls im Falle des Gleichgewichts, gleicht die Oberflächenspannung dem integral der freien energiedichte am Interface, woraus eine Beschreibung für die Oberflächenspannung abgeleitet werden kann [22].

$$\sigma = \int_{-\infty}^{\infty} \lambda\left(\frac{dC}{dn}\right)^2 = \frac{2\sqrt{2}}{3}\frac{\lambda}{\epsilon} \tag{3.7}$$

3.1.3 Wall Energy

Jaqcmin [21] postulierte eine Wandenergie der Form

$$F_{\mathrm{w}} = \int \sigma g(C) dA, \tag{3.8}$$

womit die Wandenergie nur noch eine Funktion abhängig von der Fluidzusammensetzung direkt an der Wand abhängig ist. Die resultierende natürliche Phasenfeld Randbedingung mit lokalem thermischen Gleichgewicht ist gegeben mit

$$\lambda \frac{\partial C}{\partial n_{\partial\Omega}} + f'_{\mathrm{w}}(C) = 0. \tag{3.9}$$

Mit $n_{\partial\Omega}$ als normalenrichtung auf der Wand (vgl. 3.1). Die normalenrichtung zum interface kann mit der wandnormale und wand tangentiale Richtung auf der Wand beschrieben werden.

$$n = n_{\partial\Omega} \cos(\theta_{\mathrm{e}}) + \tau_{\partial\Omega} \sin(\theta_{\mathrm{e}}). \tag{3.10}$$

Anschließend kann für den ersten Term aus Gleichung 3.9 mit den Gleichungen 3.10, 3.6 und 3.7 wie folgt erstellt werden

$$\lambda \frac{\partial C}{\partial n_{\partial\Omega}} = \underbrace{\frac{3}{4}\sigma\left(1 - C^2\right)\cos\theta_{\mathrm{e}}}_{=:-f'_{\mathrm{w}}(C)}. \tag{3.11}$$

Daraus lässt sich eine Funktion für die Wandenergiedichte nach Integration ableiten[22][19].

$$f_{\mathrm{w}}(C) = -\sigma\cos\theta_e \frac{C(3 - C^2)}{4} + \frac{\sigma_{S_L} + \sigma_{S_V}}{2} \tag{3.12}$$

Ist nur eine der Phasen anwesend, gibt diese Gleichung auch nur die jeweilige Oberflächenspannung zurück. Yue et al. [38] weißt jedoch darauf hin, dass diese Beschreibung der Wandenergie für Gleichgewichtskontaktwinkel nahe $0°$ oder $180°$ nur schwer zu reproduzieren ist und das Modell nicht in der Lage ist precursor films zu handhaben.

3.2 Cahn-Hillard Navier Stokes Equations

Die gekoppelten Cahn-Hillard Navier Stokes Gleichungen sind gegeben mit

$$\partial_t C + \nabla \cdot (C\mathbf{u}) = -\nabla \cdot \mathbf{J} \tag{3.13}$$

$$\nabla \cdot \mathbf{u} = 0 \tag{3.14}$$

$$\partial_t(\rho\mathbf{u}) + \nabla \cdot (\rho\mathbf{u}\mathbf{u}) = -\nabla\tilde{p} + \nabla\tau - \nabla \cdot (\mathbf{u}\mathbf{J}) - \phi\nabla C + \mathbf{f}_{\mathrm{b}} \tag{3.15}$$

Darin ist $\tilde{p}$ ein modifizierter Druck, der aus dem Korteweg tensor entsteht, um die Kapillarität zu berücksichtigen. Die Annahme eines Newtonschen Fluids gilt $\tau = 2\mu\mathrm{dev}\mathbf{D}$ mit $\mathbf{D} = 1/2[\nabla\mathbf{u} + (\nabla\mathbf{u})^{\mathrm{T}}]$ als Deformationstensor. Weiter ist die Dichte ρ und viskosität μ volumetrisch gemittelt mit

$$\rho = \frac{1 + C}{2}\rho_1 + \frac{1 + C}{2}\rho_2. \tag{3.16}$$

Darin sind die suffixe 1 und 2 Markierungen für die jeweiligen Phasen. Die Viskosität wird analog berechnet. Der Term $-\nabla \cdot (\mathbf{u}\mathbf{J})$ ist notwendig, um die thermische consistenz zu gewährleisten [14]. $\mathbf{J}$ ist der phase-field flux und nach Landau und Lifshitz gilt cite $\mathbf{J} = -M\nabla\phi$

4 Case Setup

To save computational effort, the axisymmetry is exploited in the simulation of the capillary, and only a wedge is simulated. The angle of the wedge is $5°$. Furthermore, water is assumed as the liquid medium and air as the gaseous medium, both at $25°$ Celsius. The corresponding material properties are listed in the following table.

Table 4.1: Physical properties

fluid	density ($\frac{kg}{m^3}$)	kinematic viscosity $\frac{m^2}{s}$
water	1000	$1.00E-06$
air	1	$1.00E-05$

insert table

The surface tension between water and air is $0.072N/m$, and the interface thickness ϵ was chosen to be approximately $1.7nm$, corresponding to the physical interface thickness. Mobility is a factor in the phase-field simulation that is difficult to determine. Jacqmin [21] suggested an asymptotic behavior for κ of

$$\kappa = \mathcal{O}(\epsilon^{\delta}) \tag{4.1}$$

and showed that $1 \leq \delta < 2$. For this work, a value of $\kappa = 1.6 \times 10^{-18}$ was used.

add checcks which were made; Viscosity scheme, probes, funkysetfields, preconditioner, boundary conditions, n cores decomposition

Simulations were conducted for various contact angles to investigate the influence of capillary rise depending on the contact angle. The initial conditions for each of these simulations were the same. The computational grid was chosen such that the elements in the axial direction.

elaborate

In Figure 4.1, both the dimensions of the wedge and the names of the surfaces that have been assigned with boundary conditions are shown. Furthermore, it can be seen which part of the capillary is already filled with water (blue area) and which part is filled with air (gray area). The surfaces labeled `front` and `back` represent the opposing faces

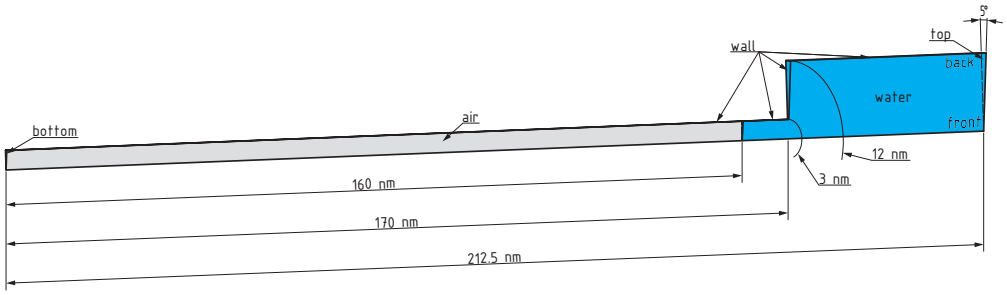

Figure 4.1: Wedge-shaped case setup

of the wedge. The surfaces `top` and `bottom` have a zero-gradient boundary condition and a pressure of $0\,Pascal$. At the wall, the no-slip condition applies, and for the order parameters, an equilibrium boundary condition is used. In this work, the usability and effects of the out-of-equilibrium boundary condition are examined as well. Additional simulations were conducted with the same setup as before, but with the activated boundary condition.

ref to chapter ooEBC

4.1 Discretization

Da es sich um eine relativ simple geometrie handelt, wurde die Geometrie direkt in der `blockMeshDict`- Datei erstellt. Die Netzdichte wurde so gewählt, dass die Kantenlänge der Kontrollvolumen $0.1nm$ entsprechen. Dadurch können mögliche Probleme durch geringe Kontaktwinkel minimiert werden. Simulationen mit großem Winkel wurden ebenfalls mit gleichem Rechnetz simuliert, um eine gute vergleichbarbeit gewährleisten zu können.

we used an other geometry. How do i write it then?new image with new text?

One of the significant advantages of simulation is the ability to examine areas that are difficult or impossible to measure in reality. For each of the simulations, several values were extracted to assist in the later evaluation and assessment of the simulation. These include the acting viscous or capillary forces.

5 Validation

The `phaseFieldFoam`- Solver

src

- Moradi2021 Laplace Test

bodziony2023 Cai2015, woerner2021, Samkhaniani2021, holtzinger, marianna?, hagg?(sogar mit wedge und amr)

6 Results

The Position of the meniskus was exported with paraview in the decomposed state. The position was then extracted with a python script.Probe data was preprocessed as well and several computations for eval of simulations. Plots were generated with matplotlib?; Start of real results with an overview when what where. Maybe work with normalized data?

7 Outlook

- complex geometry
- temperature dependent capillary rise?
- surfactants and capillary rise?
- more fluids with other viscosisties

Bibliography

[1] J. M. Bell and F. K. Cameron. “The Flow of Liquids through Capillary Spaces”. In: *The Journal of Physical Chemistry* 10.8 (Nov. 1, 1906), pp. 658–674. ISSN: 0092-7325, 1541-5740. DOI: 10.1021/j150080a005. URL: https://pubs.acs.org/doi/abs/10.1021/j150080a005 (visited on 10/05/2023).

[2] T.D Blake and J.M Haynes. “Kinetics of Displacement”. In: *Journal of Colloid and Interface Science* 30.3 (July 1969), pp. 421–423. ISSN: 00219797. DOI: 10.1016/0021-9797(69)90411-1. URL: https://linkinghub.elsevier.com/retrieve/pii/0021979769904111 (visited on 10/05/2023).

[3] Terence D. Blake. “The Physics of Moving Wetting Lines”. In: *Journal of Colloid and Interface Science* 299.1 (July 2006), pp. 1–13. ISSN: 00219797. DOI: 10.1016/j.jcis.2006.03.051. URL: https://linkinghub.elsevier.com/retrieve/pii/S0021979706002463 (visited on 10/05/2023).

[4] C.H. Bosanquet. “LV. *On the Flow of Liquids into Capillary Tubes*”. In: *The London, Edinburgh, and Dublin Philosophical Magazine and Journal of Science* 45.267 (Mar. 1923), pp. 525–531. ISSN: 1941-5982, 1941-5990. DOI: 10.1080/14786442308634144. URL: https://www.tandfonline.com/doi/full/10.1080/14786442308634144 (visited on 10/05/2023).

[5] Hans-Jürgen Butt, Karlheinz Graf, and Michael Kappl. *Physics and Chemistry of Interfaces*.

[6] Xuan Cai et al. “Numerical Simulation of Wetting Phenomena with a Phase-Field Method Using OpenFOAM®”. In: *Chemical Engineering & Technology* 38.11 (Nov. 2015), pp. 1985–1992. ISSN: 0930-7516, 1521-4125. DOI: 10.1002/ceat.201500089. URL: https://onlinelibrary.wiley.com/doi/10.1002/ceat.201500089 (visited on 10/05/2023).

[7] A. Carlson, M. Do-Quang, and G. Amberg. “Dissipation in Rapid Dynamic Wetting”. In: *Journal of Fluid Mechanics* 682 (Sept. 10, 2011), pp. 213–240. ISSN: 0022-1120, 1469-7645. DOI: 10.1017/jfm.2011.211. URL: https://www.cambridge.org/core/product/identifier/S0022112011002114/type/journal_article (visited on 10/05/2023).

[8] Andreas Carlson. “Capillarity and Dynamic Wetting”. KTH Royal Institute of Technology, 2012.

[9] Li Chen et al. “A Critical Review of the Pseudopotential Multiphase Lattice Boltzmann Model: Methods and Applications”. In: *International Journal of Heat and Mass Transfer* 76 (Sept. 2014), pp. 210–236. ISSN: 00179310. DOI: 10.1016/j.ijheatmasstransfer.2014.04.032. URL: https://linkinghub.elsevier.com/retrieve/pii/S0017931014003378 (visited on 10/10/2023).

[10] R. G. Cox. “The Dynamics of the Spreading of Liquids on a Solid Surface. Part 1. Viscous Flow”. In: *Journal of Fluid Mechanics* 168 (-1 July 1986), p. 169. ISSN: 0022-1120, 1469-7645. DOI: 10.1017/S0022112086000332. URL: http://www.journals.cambridge.org/abstract_S0022112086000332 (visited on 10/05/2023).

[11] Deeptayan Datta et al. “Early-Stage Liquid Infiltration in Nanoconfinements”. In: *Langmuir* 39.9 (Mar. 7, 2023), pp. 3301–3311. ISSN: 0743-7463, 1520-5827. DOI: 10.1021/acs.langmuir.2c03154. URL: https://pubs.acs.org/doi/10.1021/acs.langmuir.2c03154 (visited on 10/05/2023).

[12] Joachim Delannoy et al. “The Dual Role of Viscosity in Capillary Rise”. In: *Soft Matter* 15.13 (2019), pp. 2757–2761. ISSN: 1744-683X, 1744-6848. DOI: 10.1039/C8SM02485E. URL: http://xlink.rsc.org/?DOI=C8SM02485E (visited on 10/05/2023).

[13] D. I. Dimitrov, A. Milchev, and K. Binder. “Capillary Rise in Nanopores: Molecular Dynamics Evidence for the Lucas-Washburn Equation”. In: *Physical Review Letters* 99.5 (July 31, 2007), p. 054501. ISSN: 0031-9007, 1079-7114. DOI: 10.1103/PhysRevLett.99.054501. URL: https://link.aps.org/doi/10.1103/PhysRevLett.99.054501 (visited on 10/05/2023).

[14] Hang Ding, Peter D.M. Spelt, and Chang Shu. “Diffuse Interface Model for Incompressible Two-Phase Flows with Large Density Ratios”. In: *Journal of Computational Physics* 226.2 (Oct. 2007), pp. 2078–2095. ISSN: 00219991. DOI: 10.1016/j.jcp.2007.06.028. URL: https://linkinghub.elsevier.com/retrieve/pii/S0021999107002793 (visited on 10/05/2023).

[15] Michael Dreyer, Antonio Delgado, and Hans-Joseph Path. “Capillary Rise of Liquid between Parallel Plates under Microgravity”. In: *Journal of Colloid and Interface Science* 163.1 (Mar. 1994), pp. 158–168. ISSN: 00219797. DOI: 10.1006/jcis.1994.1092. URL: https://linkinghub.elsevier.com/retrieve/pii/S0021979784710927 (visited on 10/05/2023).

[16] Mathis Fricke et al. “An Analytical Study of Capillary Rise Dynamics: Critical Conditions and Hidden Oscillations”. In: *Physica D: Nonlinear Phenomena* 455 (Dec. 2023), p. 133895. ISSN: 01672789. DOI: 10.1016/j.physd.2023.133895. arXiv: 2305.05939 [physics]. URL: http://arxiv.org/abs/2305.05939 (visited on 10/05/2023).

[17] N. Fries and M. Dreyer. “The Transition from Inertial to Viscous Flow in Capillary Rise”. In: *Journal of Colloid and Interface Science* 327.1 (Nov. 2008), pp. 125–128. ISSN: 00219797. DOI: 10.1016/j.jcis.2008.08.018. URL: https://linkinghub.elsevier.com/retrieve/pii/S0021979708009661 (visited on 10/05/2023).

[18] Daniel Hagg. “Direkte numerische Simulation von transientem Benetzungsverhalten in komplexen Dichtspaltgeometrien unter Verwendung von phaseFieldFoam”. In: (2019). In collab. with Bettina Frohnapfel et al. DOI: 10.5445/IR/1000145948. URL: https://publikationen.bibliothek.kit.edu/1000145948 (visited on 10/05/2023).

[19] Michael Holzinger and TU Darmstadt. *Direct Numerical Simulation of Dynamic Droplet Wetting on Superhydrophobic Substrates by Means of a Diffuse-Interface Phase-Field Method Using OpenFOAM*. In collab. with Technical University Of Darmstadt. Technical University of Darmstadt, 2021. DOI: 10.48328/TUDATALIB-473. URL: https://tudatalib.ulb.tu-darmstadt.de/handle/tudatalib/2689 (visited on 10/05/2023).

[20] Chun Huh and L.E Scriven. “Hydrodynamic Model of Steady Movement of a Solid/Liquid/Fluid Contact Line”. In: *Journal of Colloid and Interface Science* 35.1 (Jan. 1971), pp. 85–101. ISSN: 00219797. DOI: 10.1016/0021-9797(71)90188-3. URL: https://linkinghub.elsevier.com/retrieve/pii/0021979771901883 (visited on 10/05/2023).

[21] David Jacqmin. “Calculation of Two-Phase Navier–Stokes Flows Using Phase-Field Modeling”. In: *Journal of Computational Physics* 155.1 (Oct. 1999), pp. 96–127. ISSN: 00219991. DOI: 10.1006/jcph.1999.6332. URL: https://linkinghub.elsevier.com/retrieve/pii/S0021999199963325 (visited on 10/05/2023).

[22] David Jacqmin. “Contact-Line Dynamics of a Diffuse Fluid Interface”. In: *Journal of Fluid Mechanics* 402 (Jan. 10, 2000), pp. 57–88. ISSN: 0022-1120, 1469-7645. DOI: 10.1017/S0022112099006874. URL: https://www.cambridge.org/core/product/identifier/S0022112099006874/type/journal_article (visited on 10/05/2023).

[23] F. Jamshidi et al. “On Suitability of Phase-Field and Algebraic Volume-of-Fluid OpenFOAM® Solvers for Gas–Liquid Microfluidic Applications”. In: *Computer Physics Communications* 236 (Mar. 2019), pp. 72–85. ISSN: 00104655. DOI: 10.1016/j.cpc.2018.10.015. URL: https://linkinghub.elsevier.com/retrieve/pii/S0010465518303631 (visited on 10/05/2023).

[24] Cahn John W. and Hillard John E. “Free Energy of a Nonuniform System. I. Interfacial Free Energy”. In: 28.2 (Feb. 1958). DOI: 10.1063/1.1744102.

[25] Uğis Lācis et al. “Nanoscale Sheared Droplet: Volume-of-Fluid, Phase-Field and No-Slip Molecular Dynamics”. In: *Journal of Fluid Mechanics* 940 (June 10, 2022), A10. ISSN: 0022-1120, 1469-7645. DOI: 10.1017/jfm.2022.219. URL: https://

www.cambridge.org/core/product/identifier/S0022112022002191/type/journal_article (visited on 10/09/2023).

[26] Richard Lucas. "Ueber das Zeitgesetz des kapillaren Aufstiegs von Flüssigkeiten". In: *Kolloid-Zeitschrift* 23.1 (July 1918), pp. 15–22. ISSN: 0303-402X, 1435-1536. DOI: 10.1007/BF01461107. URL: http://link.springer.com/10.1007/BF01461107 (visited on 10/05/2023).

[27] G. Martic et al. "A Molecular Dynamics Simulation of Capillary Imbibition". In: *Langmuir* 18.21 (Oct. 1, 2002), pp. 7971–7976. ISSN: 0743-7463, 1520-5827. DOI: 10.1021/la020068n. URL: https://pubs.acs.org/doi/10.1021/la020068n (visited on 10/05/2023).

[28] Alireza Mohammad Karim. "A Review of Physics of Moving Contact Line Dynamics Models and Its Applications in Interfacial Science". In: *Journal of Applied Physics* 132.8 (Aug. 28, 2022), p. 080701. ISSN: 0021-8979, 1089-7550. DOI: 10.1063/5.0102028. URL: https://pubs.aip.org/jap/article/132/8/080701/2837259/A-review-of-physics-of-moving-contact-line (visited on 10/05/2023).

[29] D Quéré. "Inertial Capillarity". In: *Europhysics Letters (EPL)* 39.5 (Sept. 1, 1997), pp. 533–538. ISSN: 0295-5075, 1286-4854. DOI: 10.1209/epl/i1997-00389-2. URL: https://iopscience.iop.org/article/10.1209/epl/i1997-00389-2 (visited on 10/05/2023).

[30] Élfego Ruiz-Gutiérrez et al. "The Long Cross-over Dynamics of Capillary Imbibition". In: *Journal of Fluid Mechanics* 939 (May 25, 2022), A39. ISSN: 0022-1120, 1469-7645. DOI: 10.1017/jfm.2022.248. URL: https://www.cambridge.org/core/product/identifier/S0022112022002488/type/journal_article (visited on 10/05/2023).

[31] Robert Siegel. "Transient Capillary Rise in Reduced and Zero-Gravity Fields". In: *Journal of Applied Mechanics* 28.2 (June 1, 1961), pp. 165–170. ISSN: 0021-8936, 1528-9036. DOI: 10.1115/1.3641647. URL: https://asmedigitalcollection.asme.org/appliedmechanics/article/28/2/165/385908/Transient-Capillary-Rise-in-Reduced-and (visited on 10/05/2023).

[32] Michael Stange, Michael E. Dreyer, and Hans J. Rath. "Capillary Driven Flow in Circular Cylindrical Tubes". In: *Physics of Fluids* 15.9 (Sept. 1, 2003), pp. 2587–2601. ISSN: 1070-6631, 1089-7666. DOI: 10.1063/1.1596913. URL: https://pubs.aip.org/pof/article/15/9/2587/450889/Capillary-driven-flow-in-circular-cylindrical (visited on 10/05/2023).

[33] J. D. Van Der Waals. "The Thermodynamic Theory of Capillarity under the Hypothesis of a Continuous Variation of Density". In: *Journal of Statistical Physics* 20.2 (Feb. 1979), pp. 200–244. ISSN: 0022-4715, 1572-9613. DOI: 10.1007/BF01011514. URL: http://link.springer.com/10.1007/BF01011514 (visited on 10/05/2023).

[34] O. V. Voinov. “Hydrodynamics of Wetting”. In: *Fluid Dynamics* 11.5 (1977), pp. 714–721. ISSN: 0015-4628, 1573-8507. DOI: 10.1007/BF01012963. URL: http://link.springer.com/10.1007/BF01012963 (visited on 10/05/2023).

[35] Edward W. Washburn. “The Dynamics of Capillary Flow”. In: *Physical Review* 17.3 (Mar. 1, 1921), pp. 273–283. ISSN: 0031-899X. DOI: 10.1103/PhysRev.17.273. URL: https://link.aps.org/doi/10.1103/PhysRev.17.273 (visited on 10/05/2023).

[36] Pingkeng Wu, Alex D. Nikolov, and Darsh T. Wasan. “Capillary Rise: Validity of the Dynamic Contact Angle Models”. In: *Langmuir* 33.32 (Aug. 15, 2017), pp. 7862–7872. ISSN: 0743-7463, 1520-5827. DOI: 10.1021/acs.langmuir.7b01762. URL: https://pubs.acs.org/doi/10.1021/acs.langmuir.7b01762 (visited on 10/05/2023).

[37] P. Yue and J. J. Feng. “Can Diffuse-Interface Models Quantitatively Describe Moving Contact Lines?” In: *The European Physical Journal Special Topics* 197.1 (Aug. 2011), pp. 37–46. ISSN: 1951-6355, 1951-6401. DOI: 10.1140/epjst/e2011-01434-y. URL: http://link.springer.com/10.1140/epjst/e2011-01434-y (visited on 10/05/2023).

[38] Pengtao Yue and James J. Feng. “Wall Energy Relaxation in the Cahn–Hilliard Model for Moving Contact Lines”. In: *Physics of Fluids* 23.1 (Jan. 1, 2011), p. 012106. ISSN: 1070-6631, 1089-7666. DOI: 10.1063/1.3541806. URL: https://pubs.aip.org/pof/article/23/1/012106/937545/Wall-energy-relaxation-in-the-Cahn-Hilliard-model (visited on 10/05/2023).

[39] Pengtao Yue, Chunfeng Zhou, and James J. Feng. “Sharp-Interface Limit of the Cahn–Hilliard Model for Moving Contact Lines”. In: *Journal of Fluid Mechanics* 645 (Feb. 25, 2010), pp. 279–294. ISSN: 0022-1120, 1469-7645. DOI: 10.1017/S0022112009992679. URL: https://www.cambridge.org/core/product/identifier/S0022112009992679/type/journal_article (visited on 10/05/2023).

[40] B.V. Zhmud, F. Tiberg, and K. Hallstensson. “Dynamics of Capillary Rise”. In: *Journal of Colloid and Interface Science* 228.2 (Aug. 2000), pp. 263–269. ISSN: 00219797. DOI: 10.1006/jcis.2000.6951. URL: https://linkinghub.elsevier.com/retrieve/pii/S0021979700969510 (visited on 10/05/2023).